JCB Article

Keratins modulate colonocyte electrolyte transport via protein mistargeting

Diana M. Toivola,[1,2] Selvi Krishnan,[4] Henry J. Binder,[3] Satish K. Singh,[4] and M. Bishr Omary[1,2]

[1]Palo Alto VA Medical Center, Palo Alto, CA 94304
[2]Stanford University School of Medicine Digestive Disease Center, Stanford, CA 94305
[3]Yale University School of Medicine, New Haven, CT 06520
[4]Boston Medical Center, Boston, MA 02118

The function of intestinal keratins is unknown, although keratin 8 (K8)–null mice develop colitis, hyperplasia, diarrhea, and mistarget jejunal apical markers. We quantified the diarrhea in K8-null stool and examined its physiologic basis. Isolated crypt-units from K8-null and wild-type mice have similar viability. K8-null distal colon has normal tight junction permeability and paracellular transport but shows decreased short circuit current and net Na absorption associated with net Cl secretion, blunted intracellular Cl/HCO_3-dependent pH regulation, hyperproliferation and enlarged goblet cells, partial loss of the membrane-proximal markers H,K-ATPase-β and F-actin, increased and redistributed basolateral anion exchanger AE1/2 protein, and redistributed Na-transporter ENaC-γ. Diarrhea and protein mistargeting are observed 1–2 d after birth while hyperproliferation/inflammation occurs later. The AE1/2 changes and altered intracellular pH regulation likely account, at least in part, for the ion transport defects and hyperproliferation. Therefore, colonic keratins have a novel function in regulating electrolyte transport, likely by targeting ion transporters to their cellular compartments.

Introduction

Keratin polypeptides 7, 8, 18, 19, and 20 are the cytoskeletal intermediate filament (IF) proteins of intestinal epithelia (Moll et al., 1982; Zhou et al., 2003). Keratin 8 (K8) is the major type II keratin in digestive organs, including the small and large intestine, where it forms obligate noncovalent heteropolymers with one or more of the type I keratins K18, K19, or K20 depending on the cell and tissue involved (Coulombe and Omary, 2002). K8 ablation results in 50% embryolethality in FVB/n mice and is accompanied by female sterility, colonic hyperplasia, colitis, rectal prolapse, loose stools (Baribault et al., 1993, 1994; Jaquemar et al., 2003), and mistargeting of jejunal apical membrane proteins (Ameen et al., 2001). In addition, K8-null mice have partially distorted hepatic and pancreatic morphology (Loranger et al., 1997; Toivola et al., 1998, 2001) and are markedly predisposed to various forms of liver (Loranger et al., 1997; Toivola et al., 1998; Caulin et al., 2000; Zatloukal et al., 2000), but not pancreatic, injury (Toivola et al., 2000). Since K8 stabilizes its partner K18, K19, and K20 proteins, K8-null mouse jejunal enterocytes are essentially devoid of cytoplasmic IF proteins except in crypt and goblet cells, which express low levels of K7 (Baribault et al., 1994; Ameen et al., 2001).

The major function of K8/18 in the liver is protection from mechanical and nonmechanical forms of stress (Omary et al., 2002), which was initially noted for the epidermal keratins K5/14 (Fuchs and Weber, 1994). This function is also noted in oral/esophageal (K4/13) and ocular (K3/12) keratins and is supported by the accumulating number of keratin and corresponding cell type–specific diseases (Irvine and McLean, 1999; Ku et al., 2003a). In contrast, keratin function in the intestine is poorly understood, although the K8-null mouse phenotype suggests a potential role in cell growth, differentiation, or targeting of proteins to the apical compartment.

The water content of stool is controlled by intestinal fluid absorption and secretion, which in turn is regulated mainly by Na and Cl transport across the apical membrane of small intestinal and colonic epithelial cells (Barrett and Keely,

D.M. Toivola and S. Krishnan contributed equally to this work.

Address correspondence to Bishr Omary, Palo Alto VA Medical Center, 3801 Miranda Ave., Mail code 154J, Palo Alto, CA 94304. Fax: (650) 852-3259.

Key words: ion transport; diarrhea; intestine; intermediate filaments; cytoskeleton

Abbreviations used in this paper: CFTR, cystic fibrosis transmembrane receptor; DRA, down-regulated in adenoma; IF, intermediate filament; K, keratin; NHE3, Na/H exchanger 3; pH_i, intracellular pH.

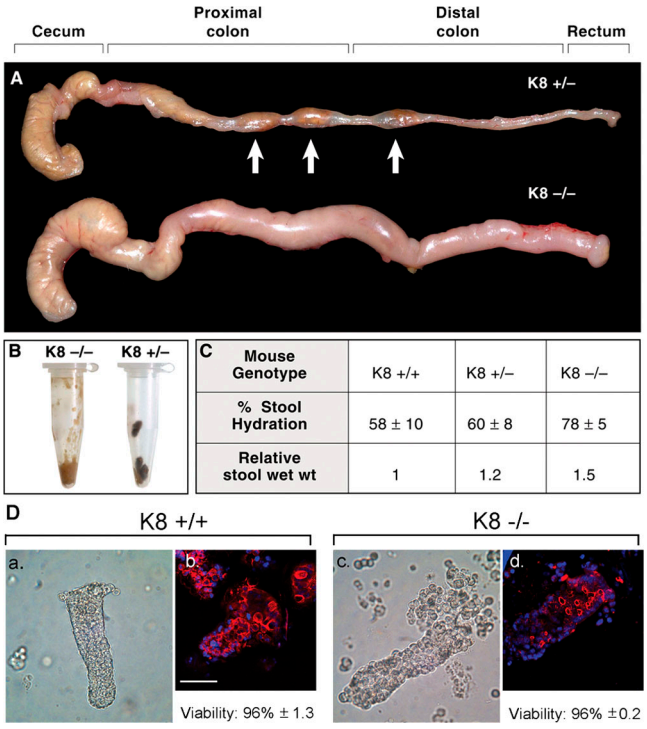

Figure 1. **Gross colonic morphology and stool characterization of K8 mouse genotypes.** (A) The entire colon from cecum to rectum was excised from K8+/− and K8−/− mice. Note the thicker K8−/− colon compared with the K8+/− colon (which is identical to K8+/+) through which stool pellets (arrows) can be seen. (B) K8−/− stool is loose as compared with K8+/− stool pellets. (C) Percent stool hydration ± SD and relative stool wet weight (normalized to K8+/+). $P < 0.0001$ (K8−/− vs. WT); $P < 0.0002$ (K8−/− vs. K8+/−) when comparing stool percent hydration. (D) Colonocytes/crypt-units were isolated from K8+/+ (a and b) and K8−/− (c and d) colon and shown as phase contrast images (a and c) or after immunostaining for K8/18 (red) and nuclei (blue; b and d). Viability was determined by measuring the percent of LDH leakage and is given as average of three experiments ± SD. Bar, 50 μm (for b and d).

2000; Kere and Hoglund, 2000; Kunzelmann and Mall, 2002). Active Na absorption can occur through electrogenic transport (e.g., the epithelial Na channel ENaC) or through electroneutral NaCl absorption, generally a result of coupled Na-H (Na/H exchanger 3 [NHE3]) and Cl/HCO_3 (down-regulated in adenoma [DRA]) exchangers. Cl absorption can be passive along favorable electrochemical gradients, or active such as electroneutral Cl/HCO_3 exchange (e.g., DRA) or NaCl absorption (NHE3 in concert with DRA). The cystic fibrosis transmembrane receptor (CFTR), and the basolateral anion exchanger 2 (AE2; Cl/HCO_3) are also important in maintaining Na/Cl balance (Binder and Sandle, 1994; Kere and Hoglund, 2000; Kunzelmann and Mall, 2002). Epithelial cell polarity and the cytoskeletal microfilament and microtubule maintenance of such polarity are known to be important for vectorial ion transport (Hofer et al., 1998), while any potential role for keratin IF is unknown and has not been studied. Although diarrhea was reported in qualitative terms in K8-null mice (Baribault et al., 1994), its pathogenesis and biological basis are unknown. To address these issues, we used K8-null mice to test the hypothesis that keratins may play a role in colonic electrolyte transport.

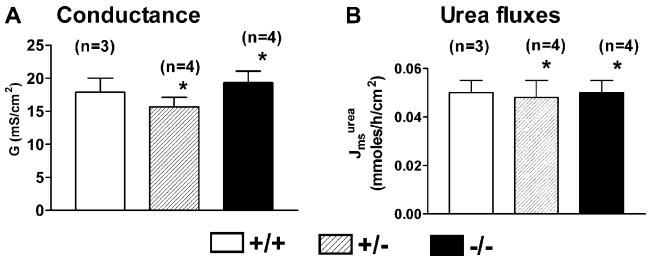

Figure 2. **Conductance and paracellular transport of [^{14}C]urea in distal colon of K8+/+, +/−, and −/− mice.** Distal colon from K8+/+, +/−, or −/− mice was mounted in lucite chambers. Conductance was determined from short circuit current (I_{sc}) and potential difference (P.D.). Conductance (A) and urea fluxes, J_{ms}^{urea} (B), represent the average of two 15-min intervals and are expressed as mean ± SEM. *n*, number of tissues studied in each group. *, not significantly different from K8+/+.

Results

Diarrhea in K8-null mice associates with abnormal colonic active Na and Cl transport but is unrelated to altered paracellular transport

Since previous studies only mentioned that K8-null mice have watery stool (Baribault et al., 1994), we first quantified the diarrhea in K8−/−, K8+/−, and K8+/+ mice. K8−/− mice produce loose stool (Fig. 1, A and B) and have significantly higher stool water content and lower body weight compared with K8+/+ (Fig. 1 C). Isolated colonocytes/crypt-units from K8−/− and K8+/+ mice had similar viability (96%; Fig. 1 D), and their purity was confirmed by staining using anti-keratin antibodies (Fig. 1 D) and lack of reactivity with vimentin antibodies (not depicted). This indicates that K8-null colonocytes/crypts are similar to pancreatic acinar cells (Toivola et al., 2000) as contrasted with hepatocytes (Loranger et al., 1997), in terms of their lack of fragility upon isolation.

To understand the physiologic basis of diarrhea in K8-null mice, we asked whether it could be caused by a "leaky" colonic epithelium. Conductance of colonic tissues, a measure of tight junction function, was not significantly different in all three genotypes (Fig. 2 A): 19.3 ± 1.8 (K8−/−), 15.7 ± 1.4 (K8+/−), and 17.9 ± 2.1 mS/cm^2 (K8+/+). Mucosal-to-serosal ^{14}C-urea fluxes across the distal colon, reflecting paracellular transport, were also similar in K8−/−, K8+/−, and K8+/+ mice (0.050 ± 0.005, 0.048 ± 0.007, and 0.050 ± 0.005 mmol/h/cm^2, respectively; Fig. 2 B). These observations indicate that the diarrhea of K8−/− mice is not related to altered paracellular transport or increased tight junction permeability.

Since paracellular transport is normal in K8−/− mice, we examined colonic ion transport by studying the short circuit current (I_{sc}) and active transport of Na and Cl. I_{sc} was dramatically decreased in K8−/− and K8+/− mice compared with K8+/+ mice (1.8 ± 0.4, 3.0 ± 0.6, and 5.6 ± 0.4 μEq/h/cm^2, respectively; Fig. 3 A). Net Na absorption was also markedly decreased in K8−/− and K8+/− mice compared with K8+/+ mice (1.6 ± 0.6, 3.8 ± 1.3, and 5.4 ± 0.4 μEq/h/cm^2, respectively; Fig. 3 B). Net Cl fluxes decreased significantly in K8−/− and K8+/− mice (Fig. 3 C), with reversal of net Cl movement to net Cl secretion in

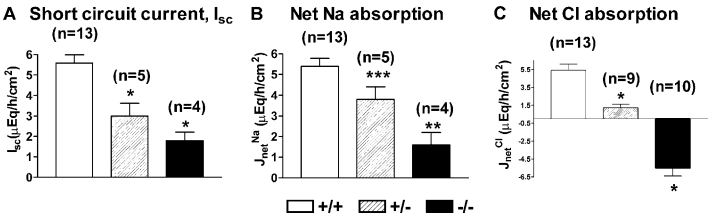

Figure 3. **Short circuit current and net Na and Cl fluxes in distal colon.** I_{sc} (A) and unidirectional mucosa-to-serosa and serosa-to-mucosa fluxes of ^{22}Na (B) and ^{36}Cl (C) were measured under voltage-clamp conditions across distal colon of K8+/+, +/−, and −/− mice bathed in normal Ringer solutions in lucite chambers. Net Na (J_{net}^{Na}) and Cl (J_{net}^{Cl}) fluxes were calculated as the difference between mucosa-to-serosa and serosa-to-mucosa fluxes between conductance-matched tissue pairs (average of two 15-min intervals expressed as mean ± SEM). *n*, number of tissue pairs studied in each group. *, $P < 0.005$; **, $P < 0.002$; ***, not significantly different (when compared with K8+/+).

K8−/− mice as compared with net Cl absorption in K8+/− and K8+/+ mice (−5.5 ± 0.9, 1.2 ± 0.4, and 5.4 ± 0.7 μEq/h/cm^2, respectively). Hence, active transport of both Na and Cl are significantly altered in K8−/− and K8+/− mice.

Na and Cl transport in WT and K8-null mice

Before embarking on studying altered Na/Cl transport in K8−/− mice, we examined baseline transport characteristics of K8+/+ mouse distal colon because little is known regarding such transport in mouse as compared with rat colon (Kunzelmann and Mall, 2002). Removal of mucosal Na abolished the I_{sc} (0.6 ± 0.7 vs. 4.0 ± 0.7 μEq/h/cm^2; Fig. 4 A), suggesting the presence of an electrogenic Na-linked absorptive transport process. Na removal from the serosal side did not alter the I_{sc} (3.7 ± 0.3 [−Na] vs. 3.6 ±0.6 μEq/h/cm^2 [+Na], not depicted, $n = 3$). However, net Cl fluxes were not significantly different upon Na removal (4.7 ± 1.8 vs. 4.9 ± 2.6 μEq/h/cm^2; Fig. 4 B). Therefore, the decrease in I_{sc} after mucosal Na removal is not related to Cl secretion, but is likely due to inhibition of electrogenic Na absorption.

We also assessed the effect of Cl removal from the serosal or mucosal side. Cl removal decreased I_{sc} significantly (2.4 ± 0.2 vs. 5.9 ± 0.5 μEq/h/cm^2; Fig. 4 C) and decreased net Na absorption (3.5 ± 0.7 vs. 5.8 ± 0.4 μEq/h/cm^2; Fig. 4 D), which indicate that electrogenic Na absorption is partially Cl dependent. However, addition of 100 μM amiloride, which inhibits the electrogenic Na transporter ENaC, failed to inhibit I_{sc} (3.8 ±1.0 [+amiloride] vs. 3.5 ±0.7 μEq/h/cm^2 [−amiloride]) and caused a limited decrease in J_{ms}^{Na} (12.7 ±2.4 [+amiloride] vs. 14.9 ±12.7 μEq/h/cm^2 [−amiloride]) (not depicted). These data suggest that K8+/+ mice have an electrogenic but amiloride-insensitive Na absorption that is partly Cl dependent, while Cl absorption is Na independent.

In contrast to findings in K8+/+ mice, mucosal Na removal in K8−/− mice resulted in a nonsignificant decrease in I_{sc} (0.5 ± 0.1 vs. 0.9 ± 0.2 μEq/h/cm^2; Fig. 4 E). Similarly, Cl removal had a minimal effect on the I_{sc} in K8−/− mice (1.2 ± 0.5 vs. 1.0 ± 0.4 μEq/h/cm^2; Fig. 4 F). Serosal Na removal did not alter I_{sc} in K8−/− mice (2.4 ± 1.3 [−Na] vs. 2.2 ±1.3 μEq/h/cm^2 [+Na], not depicted, $n = 3$). This indicates that most of the remaining Na absorption in K8−/− mice is nonelectrogenic and chloride independent.

Effect of pharmacologic agents on colonic ion transport in K8-null mice

Active Cl secretion in K8−/− mice, instead of the normal expected absorption, could result from absence of normal Cl absorption or induction of Cl secretion, or both. To test these possibilities, we first studied the effect of bumetanide, an inhibitor of the basolateral sodium-potassium-chloride

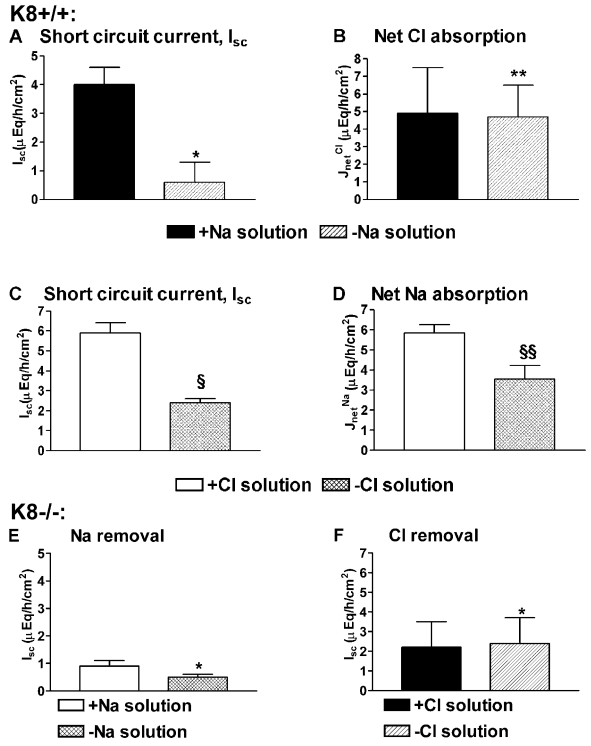

Figure 4. **Effect of external Na and Cl substitution on I_{sc} and net Na and Cl fluxes in WT and K8-null mouse colon.** (A and B) Distal colon from K8+/+ mice was mounted in lucite chambers and bathed in Na-free Ringer solution on the mucosal side and Na-containing Ringer solution on the serosal side. Unidirectional Cl fluxes were determined (−Na), and then the mucosal solution was replaced with Na-containing solution and allowed to equilibrate for 15 min, and fluxes were determined (+Na) again. (C and D) K8+/+ distal colon was bathed in Cl-free Ringer solution on the mucosal and serosal sides, and then Na fluxes were determined (−Cl) as above. Mucosal and serosal solutions were replaced with Cl-containing solution (+Cl) and fluxes were determined. Results represent an average of two time periods from five (A and B) and three (C and D) tissue pairs and are expressed as mean ± SEM. *, $P < 0.005$ compared with +Na; **, not statistically significant compared with +Na; §, $P < 0.001$ compared with +Cl; §§, $P < 0.05$ compared with +Cl. (E and F) Distal colon (in lucite chambers) from K8−/− mice bathed in Na-free or Cl-free Ringer solutions. I_{sc} was measured, and the results represent the average of two 15-min intervals determined from six tissues in each group expressed as mean ± SEM. *, not statistically significant compared with control +Na or +Cl solutions, respectively.

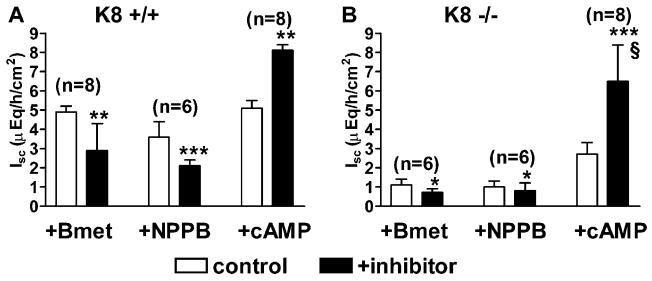

Figure 5. **Effects of transport inhibitors on I_{sc} mouse distal colon.** Distal colon (in lucite chambers) from K8+/+ (A) or K8 −/− (B) mice was bathed in normal Ringer solution and I_{sc} was measured (control). Bumetanide (Bmet, 100 μM, serosal side), NPPB (50 μM, mucosal side), or cAMP (1 mM, serosal side) was added and allowed to equilibrate for 15 min. I_{sc} was measured for two additional periods (+inhibitor). Results represent the average of two successive intervals (expressed as mean ± SEM). *n*, number of tissues studied in each group. *, not significant compared with control; **, $P < 0.001$ compared with control; ***, $P < 0.05$ compared with control. §, change in K8-null I_{sc} after cAMP addition is not significantly different from K8 WT (using paired *t* test).

cotransporter (Na-K-2Cl), that blocks basolateral Cl uptake and consequently inhibits Cl secretion. Bumetanide significantly decreased I_{sc} in K8+/+ (4.9 ± 0.3 vs. 2.9 ± 1.4 μEq/h/cm^2; Fig. 5 A) but not in K8−/− (1.1 ± 0.3 vs. 0.7 ± 0.2 μEq/h/cm^2; Fig. 5 B) mice. Similarly, NPPB, a Cl channel blocker, had a minimal effect on I_{sc} in K8−/− mice (1.0 ± 0.3 vs. 0.8 ± 0.4 μEq/h/cm^2, Fig. 5 B) but significantly decreased I_{sc} in K8+/+ mice (3.6 ± 0.8 vs. 2.1 ± 0.3 μEq/h/cm^2; Fig. 5 A). Hence, basolateral Na-K-2Cl is likely to be at least one target that is affected in K8-null mice.

Since Na and Cl absorption are impaired in K8−/− mice along with a net Cl secretion, the apical membrane in the tubular crypt cells, where secretion takes place, might be altered. To test this, we studied the ability of dibutyryl cAMP to stimulate active Cl secretion. Addition of cAMP caused significant but comparable I_{sc} increases in K8+/+ and K8−/− mice (3.0 ± 0.5 and 3.8 ± 0.67 μEq/h/cm^2, respectively; Fig. 5, A and B). Therefore, parallel increases in I_{sc} in response to cAMP suggest that crypt cell function in K8−/− colon is intact.

Altered distribution of epithelial markers in K8-null distal colon

Given the dramatic differences in colonic transport in K8-null versus WT mice, we compared the histologic and ultrastructural features of K8 WT and null mouse colons. The colorectal hyperplasia in K8−/− mice (Baribault et al., 1994) is supported by the presence of frequent mitotic enterocytes (Fig. 6 B). In addition, PCNA expression is increased in K8-null versus K8+/− or WT colons (Fig. 7 A). The lumen in some areas of K8−/− colons contains some sloughed enterocytes (Fig. 6 B) that partially mask what normally appears as a flat epithelium (Fig. 6 A). Ultrastructurally, K8−/− and WT enterocytes are similar, having normal-sized microvilli while surface goblet cells in K8−/− colon are 1.4-fold larger in K8+/+ colon (1.64 ± 0.52 vs. 1.19 ± 0.55 μm^2/goblet cell, respectively [$P = 0.012$]; Fig. 6, C and D). Also, K8−/− surface goblet cells have larger

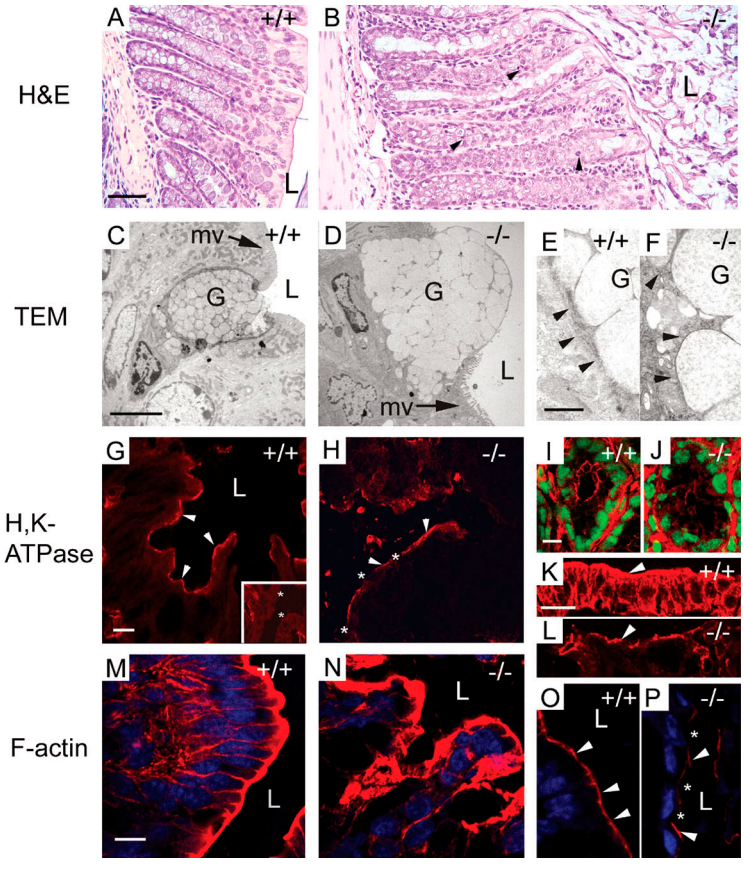

Figure 6. **Histologic, ultrastructural, and staining analysis of K8+/+ and −/− mouse distal colon.** K8+/+ and K8−/− distal colons were fixed then stained with hematoxylin and eosin (H&E; A and B), analyzed by transmission electron microscopy (TEM; C–F), or examined by immunofluorescence single or double staining to visualize H,K-ATPase (red, G–J; with nuclei stained green in I and J), K19 (red, K and L), F-actin (red, M–P; with nuclei stained blue in M–P). (A and B) Arrowheads in B highlight mitotic cells. Bar, 50 μm. L, lumen. (C–F) Arrowheads in E and F highlight keratin bundles that are present in K8+/+ (E) but absent in K8 −/− (F) mice. G, goblet cell; mv, microvilli. Bars: (C and D) 0.5 μm; (E and F) 0.05 μm. (G–J) H,K-ATPase in K8+/+ is uniformly distributed at the apical membrane of distal colon enterocytes (arrowheads in G) but is absent in the proximal colon (inset of G with asterisk highlighting apical membrane). I and J show H,K-ATPase staining at the basal regions of the crypts. Bars: (G and H) 0.05 μm; (I and J) 10 μm. The Ab also stains nonepithelial cells in the submucosa. (K and L) Arrowheads highlight the luminal apical membrane. Bar, 10 μm. (M–O) Panels O and P were obtained with identical but lower confocal laser intensity than M and N in order to visualize the uniformity (arrowheads in +/+ and −/−) versus the patchiness (asterisks in −/−) of F-actin distribution. Notably, all staining (G–P) is specific since using only second-stage antibodies on colons of +/+ or −/− mice was essentially blank (not depicted). Bar, 10 μm.

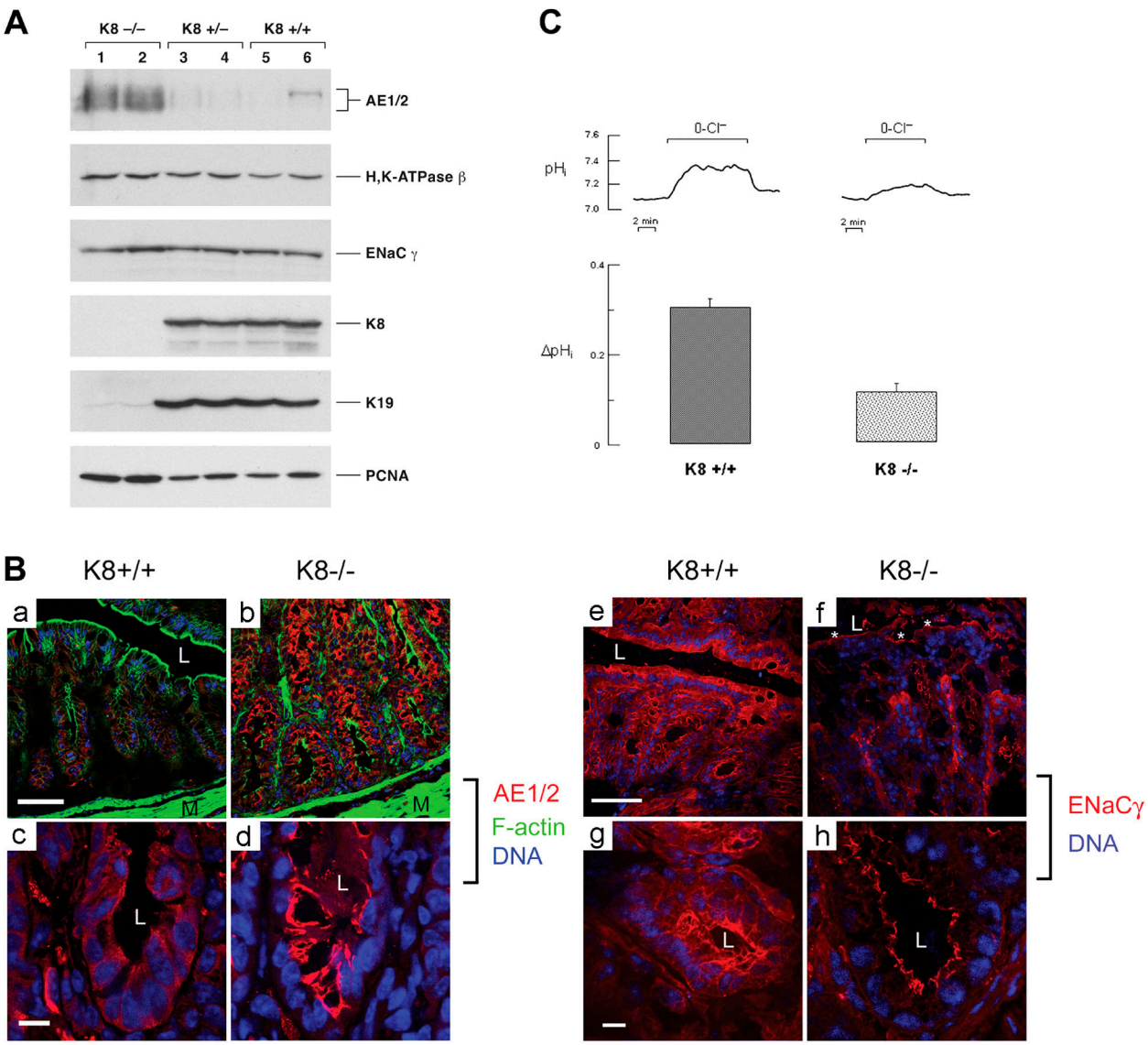

Figure 7. **Alterations in K8-null ion transporter dynamics.** (A) Immunoblot analysis of K8+/+, +/−, and −/− distal colon. Total homogenates of distal colon were loaded in equal amounts (based on protein assay; further verified by blotting using anti-tubulin Ab, not depicted) and then analyzed by blotting using antibodies to the indicated proteins. For each genotype, homogenates from two independent mice are shown. (B) Immunofluorescence staining of AE1/2 and ENaCγ in colon of K8+/+ and −/− mice. Distal colon AE1/2 (red, a–d), F-actin (green, a and b; not depicted in c and d in order to highlight the AE1/2 red staining), ENaCγ (red, e–h), and nuclei (blue, a–h) were stained. Panels c, d, g, and h show higher magnifications of the base of the tubular crypts of the corresponding a, b, d, and f panels. L, lumen; M, muscle layer. Asterisks in f highlight the apical expression of ENaCγ. Bars: (a and b) 50 μm; (c and d) 10 μm; (e and f) 50 μm; (g and h) 10 μm. (C) Surface cell pH and Cl/HCO_3 exchange activity in K8+/+ and −/− colon. Distal colon from K8+/+ and −/− mice was loaded with the pH_i-sensitive dye BCECF-AM, and individual surface epithelial cells were imaged with a low-light CCD camera. Representative pH_i (vs. time) of surface cells in K8+/+ and −/− colon during transient removal of extracellular Cl (0-Cl^-) are shown. Bar graphs show estimated Cl/HCO_3 exchange activity based on the average alkalinization observed over 5 min after Cl removal, expressed as mean ± SEM. The number of cells counted/experiments are 170/14 (K8+/+) and 120/10 (K8−/−).

mucin-containing areas per cell than K8+/+ (1.24 ± 0.42 vs. 0.89 ± 0.49 μm^2, respectively; $P < 0.003$). The K8−/− mucin droplets are irregular and lack surrounding typical keratin bundles (Fig. 6, E and F).

The epithelium of K8-null mice distal colon was evaluated using the markers H,K-ATPase-β, F-actin, and keratins. As anticipated, K7 and K18 (not depicted) and K19 (Fig. 6, K and L) remain in K8−/− as remnant keratins. The apical H,K-ATPase-β subunit had a patchy distribution in K8−/− as compared with K8+/+ colons (Fig. 6, H and G). H,K-ATPase was also uniformly present apically in K8+/+ cells in the more basal areas of the tubular crypts, but this staining was less prominent in K8−/− mice (Fig. 6, compare panels I and J). Overall H,K-ATPase protein levels were similar in K8+/+ and −/− distal colon (Fig. 7 A). F-actin was uniformly distributed at the apico-lateral domains of K8+/+ enterocytes, while in the K8−/−, lateral F-actin was absent with patchy apical staining (Fig. 6, M–P; 15% of K8-null distal colon lining had gaps in apical F-actin staining, as compared with 6% in K8+/+). These results indi-

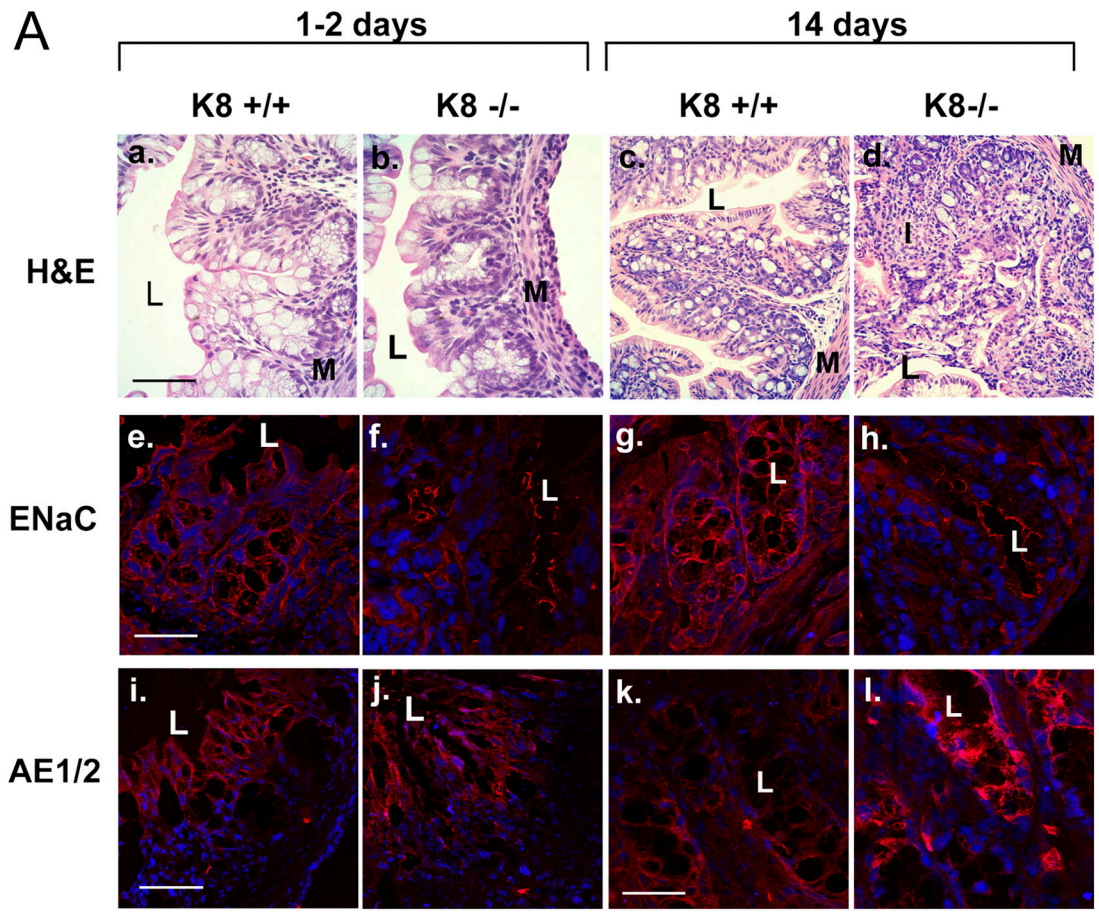

Figure 8. **Colonic histopathology, ion transporter distribution, and expression levels in WT and K8-null young mice.** (A) Colon from 1–2-d-old and 14-d-old K8+/+ and K8−/− mice was stained with hematoxylin and eosin (H&E; a–d), or examined by immunofluorescence, double staining for ENaCγ (red, e–h) and nuclei (blue, e–h) or AE1/2 (red, i–l) and nuclei (blue, e–l). M, muscle layer; I, inflammation; L, lumen. Bars: (a–d) 50 μm; (e–h) 30 μm; (i–j) 50 μm; (k and l) 30 μm. (B) Total homogenates of the entire colon from 1–2-d-old (lanes 1–6) and 14-d-old (lanes 7–12) K8+/+ and −/− were analyzed by immunoblotting using Ab to the indicated proteins. For each genotype, homogenates from three independent mice are shown.

cate that K8−/− distal colon has, in addition to increased cell proliferation, larger luminal goblet cells and mucus packets. Also, there is impaired targeting of H,K-ATPase and F-actin to apical/lateral locations.

Altered colonic expression and distribution of Na/Cl ion transporters in K8−/− distal colon

We examined the distribution and expression levels of the anion exchanger AE1/2, the Na-transporter ENaCγ, and the Na-H exchangers NHE1 and NHE3, as potential candidate transporters that could account for the alterations in Na and Cl transport. AE1/2 protein expression was significantly higher in K8−/− as compared with K8+/− or +/+ colons (Fig. 7 A). Colonic homogenates from additional mice afforded similar findings to those in Fig. 7 (marked elevation of AE1/2 protein in five of six K8−/−, one of six K8+/+, and two of six K8+/− mice; not depicted). In contrast, ENaCγ (Fig. 7 A) and NHE1/NHE3 (not depicted) levels were similar in all three mouse genotypes.

Fluorescence staining of K8−/− AE1/2 showed bright supranuclear and lateral increase (particularly in tubular crypt cells; Fig. 7 B, a–d), thereby mirroring the blotting data of Fig. 7 A. Although ENaCγ overall protein levels were not different between K8+/+ and K8−/− (Fig. 7 A), immunostaining of ENaCγ showed an altered distribution from an apical and basolateral location in K8+/+ colons to supranuclear/basal and somewhat patchy but sharp apical location (Fig. 7 B, e–h). ENaCγ was particularly strong apically in K8−/− crypt colonocytes (Fig. 7 B, h), as compared with previously described ENaC isoforms on the apical membrane of rat colonocytes (Greig et al., 2002). Therefore, the abnormal Na/Cl transport in K8−/− can be attributed to a generalized protein mistargeting that affects several ion transporters, and possibly by increased expression of the

Table I. **K8-null and K8 WT mouse body weights in grams**

Mouse age	K8−/−	K8+/+	P value
1–2 d	1.4 ± 0.2	1.6 ± 0.2	0.004
	$n = 12$	$n = 8$	
14 d	7.4 ± 1.2	8.1 ± 1.6	0.025
	$n = 8$	$n = 7$	
Adult (2–5 mo)	25.3 ± 3.3	28.5 ± 4.2	0.013
	$n = 11$	$n = 15$	

Table II. **Summary of K8-null mouse colonic phenotypes**

Feature	1–2 d	14 d	Adult
Diarrhea and lower body weight	**Yes**	**Yes**	**Yes**
Inflammation	No	**Yes**	**Yes**
Hyperproliferation	No	**Yes**	**Yes**
ENaCγ redistribution	**Yes**	**Yes**	**Yes**
AE1/2 increase	No	**Yes**	**Yes**
Apical/lateral patchy F-actin/H,K-ATPase	**Yes**	**Yes**	**Yes**

AE1/2 anion exchanger. The apparent mistargeting is not due to direct transporter–keratin association, as determined by lack of coimmunoprecipitation (not depicted).

Lack of Cl/HCO_3 function in K8 null distal colon affects intracellular pH regulation

The observed increase in AE1/2 staining in K8−/− colon suggests that epithelial acid-base handling via Cl/HCO_3 exchange activity (and thus intracellular pH [pH_i] regulation) may be altered. We examined this hypothesis by monitoring pH_i in living intact surface mucosa using the pH_i sensitive dye BCECF-AM. Over a 10-min period, the resting pH_i of surface cells was not significantly different in K8+/+ versus K8−/− colon (7.12 ± 0.02, $n = 170$ cells from 14 experiments, vs. 7.10 ± 0.02, $n = 120$ cells from 10 experiments, $P < 0.40$; not depicted). Nonetheless, because compensatory homeostatic mechanisms may mask true differences in Cl/HCO_3 exchange activity, we estimated this activity by removing Cl. In cells with plasma membrane Cl/HCO_3 exchange activity, removal of extracellular Cl reverses the exchanger, driving HCO_3 (and/or OH) into cells and causing an alkalinization that reflects plasma membrane exchange activity (Chaillet et al., 1986; Wenzl et al., 1989). As expected, extracellular Cl removal increased steady-state pH_i in K8+/+ and K8−/− colon (Fig. 7 C). However, alkalinization was greater in K8+/+ versus K8−/− colon (7.40 ± 0.02 vs. 7.21 ± 0.02, $P < 0.03$). These data, combined with the staining results, suggest that while AE1/2 protein is increased in K8−/− colon, its effective plasma membrane activity is lower than in K8+/+ colon, consistent with the observed mistargeting.

The ion transport phenotype precedes colonic hyperproliferation and inflammation

Young (1–2 and 14 d old) mice were studied to investigate the chronology of the colonic phenotypes in K8-null mice. As early as 1–2 d after birth, K8-null mice had loose stools and lower body weight compared with their WT and heterozygous littermates (Table I). Hyperproliferation (PCNA levels and histology) and inflammation (histology) were clearly discernible at 2 wk but were absent 1–2 d after birth (Fig. 8 A). F-actin and H,K-ATPase (not depicted) and ENaCγ were redistributed as early as 1–2 d after birth (Fig. 8 A, e–h). At days 1–2, AE1/2 is expressed only in the surface epithelium and not in the crypts (Fig. 8 A, i and j) with similar protein levels in WT and K8-null colons (Fig. 8 B), while by day 14, its expression extends to the crypts and becomes more prominent in K8−/− colon (Fig. 8 A, i–l). These morphological data were confirmed by immune blotting (Fig. 8 B). Therefore, lack of keratin filaments in the colon leads to altered ion transport, protein mistargeting, and diarrhea, before occurrence of hyperproliferation and inflammation.

Discussion

Overview

As a surrogate marker for intestinal keratin function, we studied the etiology of the diarrhea in K8-null mice, whose stool water content is 34% higher and whose body weight is significantly lower compared with normal mice (Fig. 1 and Table I). Since diarrhea is caused by alterations in intestinal water movement, we hypothesized that keratins may modulate epithelial barrier function and/or ion transport. In testing this hypothesis, we showed that K8-null mouse distal colon manifests (a) normal tight junction permeability (Fig. 2), (b) decreased short circuit current and Na absorption and Cl secretion instead of the typical Cl absorption (Figs. 3–5), (c) increased luminal goblet cell size and mucus content (Fig. 6), (d) generalized mistargeting of luminal and basolateral enterocyte proteins, e.g., H,K-ATPase-β and F-actin (Fig. 6), (e) increased levels of the anion exchangers AE1/2 and altered subcellular localization of AE1/2 and the electrogenic Na transporter ENaCγ (Fig. 7), and (f) blunted Cl/HCO_3 function in pH_i regulation (Fig. 7). The onset of the ion transport phenotype becomes apparent 1–2 d after birth, before onset of inflammation or hyperproliferation (Fig. 8). Overall findings are summarized in Fig. 9 and Table II.

It is not known if transport abnormalities also occur in the small intestine of K8-null mice, although near-complete absence of syntaxin and the apical markers sucrase-isomaltase, alkaline phosphatase, and CFTR were found within the upper 2/3 of the villi without affecting the crypts or the lower 1/3 of the villus (except for syntaxin; Ameen et al., 2001). The small intestinal abnormalities in K8−/− mice may also contribute to the diarrhea, despite crypt sparing and absence of histologic abnormalities. Furthermore, although diarrhea in human sucrase-isomaltase deficiency is caused by a mutation that converts it into secreted species with loss from the cell surface (Jacob et al., 2000), it is unknown if mice have a functional redundancy in such enzymatic activity. Other potential contributing factors to the diarrhea in K8-null mice include the colonic inflammation and/or goblet cell phenotype. Released products from epithelial or invading inflammatory cells could potentially alter the function of Na and/or Cl transport. However, our time course assessment (Fig. 8 and Table II) indicates that diarrhea and protein mistargeting are observed shortly after birth before onset of inflammation and hyperproliferation. Still, the onset of colitis in K8-null

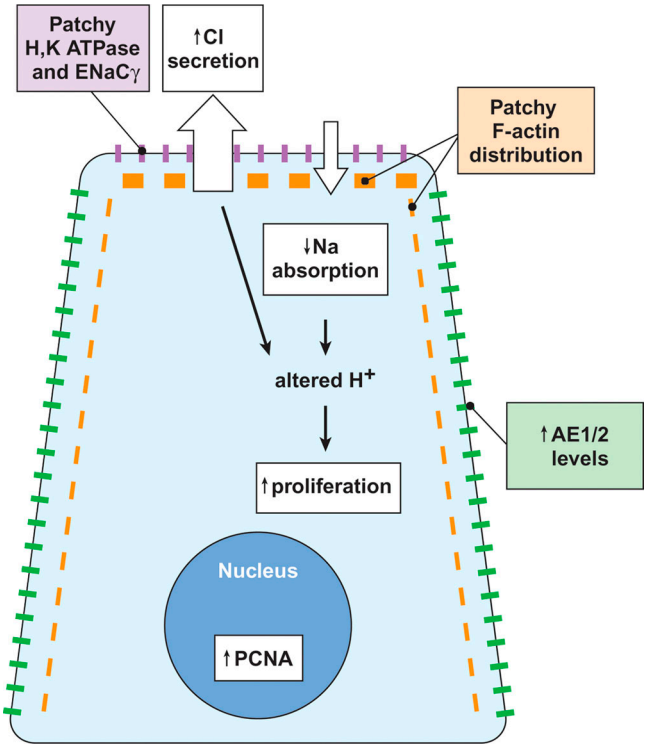

Figure 9. **Schematic summary of the K8-null mouse colonocyte phenotype.** Absence of keratins in K8-null mouse intestine results in diarrhea and then colonic hyperproliferation. The diarrhea is, at least in part, due to increased Cl secretion and decreased Na absorption. These transport abnormalities are likely related to a generalized targeting defect that is reflected by patchy distribution of H,K-ATPase, ENaCγ, and actin and increased protein levels of AE1/2. PCNA levels also increase, which is consistent with the observed colonic hyperproliferation. The increased cell proliferation is likely related to altered pH_i.

mice (between 3 and 13 d) is early among other inflammatory bowel disease genetic models that typically begin 1–4 mo after birth (e.g., IL-2−/−), with the earliest occurring in IL-7 transgenic 1–3-wk-old mice (Strober et al., 2002).

Altered ion transport in the distal colon in K8-null mice

Diarrhea may occur when ileocecal flow exceeds the maximal absorptive capacity of the colon or via an alteration in colonic absorptive functions (Binder and Sandle, 1994). The latter can be due to "leaky" tight junctions (Hosokawa et al., 1998; Kunzelmann and Mall, 2002), which does not occur in K8-null mice, since their distal colon conductance and urea fluxes were comparable to WT. Diarrhea can also result from transcellular ion transport defects in the absence of histological abnormalities, as occurs in abnormal luminal Cl/HCO_3 exchanger (DRA) leading to congenital chloride diarrhea or in secretory diarrhea caused by a defective Na/H exchanger (Kere and Hoglund, 2000; Kunzelmann and Mall, 2002). Our results show that near-total keratin absence significantly decreases I_{sc} and Na/Cl absorption; the markedly decreased I_{sc} suggests that K8-null mice have defects in electrogenic transport. Mucosal Na removal did not result in significant further decrease in I_{sc}, and there was no effect on net Cl fluxes. Cl removal also did not further decrease the I_{sc} or net Na flux, thereby supporting the absence of Cl-dependent electrogenic Na absorption in K8-null mouse distal colon. The mechanism of active Cl secretion in K8-null mice does not appear to be due to an apical Cl channel activity because the low I_{sc} values in these animals counters basal apical Cl channel function, since Cl channel function would result in elevated I_{sc} in contrast to the decreased observed I_{sc}. Rather, it appears that normal Cl absorptive processes are absent in K8-null mice. We speculate that lack of Cl absorption, in turn, is likely related to mistargeting of the Cl/HCO_3 transporter, since pH_i measurement demonstrated blunted function of this protein in K8-null distal colon despite its elevated expression as determined by staining and blot analysis.

While electroneutral Na/Cl absorption is well characterized in rat distal colon (Rajendran and Binder, 2000), little is known regarding the mouse, prompting us to define ion transport in WT mice. Although net Na and Cl fluxes were nearly equal in normal mice, thereby suggesting electroneutral Na/Cl absorption, ion substitution revealed that WT mice have an electrogenic and partially Cl-dependent Na transport, and an Na-independent electroneutral Cl absorption. The mechanism of partial Cl-dependent Na absorption is unknown, though similar Cl-dependent, electrogenic Na transport occurs in rabbit cecum (Sellin et al., 1993). I_{sc} was relatively high (5.6 μEq/h/cm^2) in WT mice considering the relatively low I_{sc} in rat distal colon (Rajendran and Binder, 2000), but similar high I_{sc} was reported in mouse and rabbit distal colon (Cuffe et al., 2002). In contrast, others (Davies et al., 1990) reported low I_{sc} (1.0 μEq/h/cm^2) and suggested the presence of electroneutral Na/Cl transport in mouse colon, although their net Na and Cl fluxes (5.1 and 6.1 μEq/h/cm^2, respectively) were similar to our findings (5.6 and 5.4 μEq/h/cm^2, respectively). The discrepancy between these studies may be due to mouse strain differences, which may also explain the relative insensitivity of K8+/+ electrogenic Na absorption to amiloride, as found by others (Cuthbert et al., 1999), though amiloride-sensitive Na absorption in mouse colon has been reported (Schulz-Baldes et al., 2001; Spicer et al., 2001; Cuffe et al., 2002).

Altered Na/Cl transport in K8-null distal colon is likely caused by mistargeting or redistribution of ion transporters

Transport proteins in the apical and basolateral cell membranes maintain the balance of transepithelial Na, Cl, and other electrolyte transport processes (Binder and Sandle, 1994). The patchy distribution of H,K-ATPase, ENaCγ, AE1/2, and F-actin in K8-null mice distal colon suggests a generalized mistargeting of proteins when keratin filaments are absent. The abnormal organization of ENaCγ, an electrogenic apical Na transporter (Ahn et al., 1999; Alvarez de la Rosa et al., 2000), offers one potential explanation for the decreased electrogenic Na uptake in K8-null mice. Similar patchiness, accompanied by significant overexpression, was also noted in the AE family of Cl/HCO_3 exchangers AE1/2 (Rajendran and Binder, 2000; Alper et al., 2002). In mouse colon, AE1/2 transport Cl into the cell in exchange for HCO_3 and are found primarily on the basolateral membrane, with highest expression in surface cells (Alper et al., 2002). Increased AE1/2 protein, if functional, may increase

intracellular Cl pools, thereby leading to Cl secretion rather than absorption. The supranuclear AE1/2 staining could involve the Golgi apparatus, since AE1/2 protein also localizes with the perinuclear Golgi where it interacts with the ankyrin/spectrin/actin cytoskeletal networks (Hofer et al., 1998). AE1/2 may also couple to Na absorption across the apical membrane via NHE2 and NHE3 exchangers (Alper et al., 2002). Interestingly, NHE3-null mice (which overexpress the apical Cl/HCO_3 transporter DRA) have diarrhea and colonic hyperproliferation (Schultheis et al., 1998), two remarkably similar findings to that observed in K8-null mice, thereby further supporting a transporter–keratin link.

The surface cell pH_i ex vivo results support our observed biochemical and distribution alterations of AE1/2. In any cell, steady-state pH_i is determined by the sum of acid-loading and acid-extruding processes (Boron, 1992). In the absence of homeostatic compensation, increased plasma membrane Cl/HCO_3 exchange will lower resting pH_i and vice versa (Chaillet et al., 1986; Wenzl et al., 1989). Steady-state pH_i in K8+/+ and K8−/− was similar despite a marked increase in AE1/2 protein in K8−/− colon. This is consistent with mistargeting of AE1/2 such that plasma membrane Cl/HCO_3 exchange activity remains effectively unchanged or homeostatic compensation that masks an increase in Cl/HCO_3 activity, or both. However, a 50% decrease in K8−/− Cl/HCO_3 exchange activity upon extracellular Cl removal is consistent with the vectorial flux data where electroneutral Cl absorption is absent from K8−/− colon. Thus, it appears that increased acid loading transport and/or metabolic H^+ production compensates for decreased plasma membrane Cl/HCO_3 exchange activity in K8−/− colon to maintain an optimal "set point" for epithelial function and proliferation.

Our study also provides a likely contributory cause of colonic hyperproliferation in K8-null mice. Another untested contributing factor may include a tropic effect induced by inflammation, since inflammation and proliferation appear to follow mistargeting (Table II). Cell cycle disturbances also occur in K8-null hepatocytes, but the genesis of such disturbances is unknown (Toivola et al., 2001). Our working model (Fig. 9) is that a change of pH_i regulation accompanies the altered transporter defects we observed coupled with the inability to alkalinize. pH alterations could then trigger cell proliferation (Bischof et al., 1996; Shrode et al., 1997), as noted in NHE3-null mice that also manifest colonic hyperplasia (Schultheis et al., 1998; Kunzelmann and Mall, 2002).

What is the function of keratins in the intestine?

There is an emerging theme that the function of keratins in simple epithelia may depend on the epithelial tissue involved rather than the specific keratin per se. This is based on findings in the liver and pancreas where K8/18 are essential for cytoprotection in the liver but dispensable in the pancreas (Coulombe and Omary, 2002). In contrast to K8-null hepatocytes, which die during isolation (Loranger et al., 1997), isolated K8-null and WT colonocytes/crypts appear to withstand isolation procedures similarly akin to K8-null pancreatic acini/acinar cells (Toivola et al., 2000). It remains to be tested if other stresses unmask a small or large intestinal cytoprotective function for keratins. However, the small intestine and colon behave differently when intestinal keratins are depleted, since the histology of K8-null mouse small intestine is normal while the large intestine has colitis and hyperproliferation (Baribault et al., 1994). This is also supported by the somewhat different molecular findings noted in the small (Ameen et al., 2001) and large intestine (present study). For example, K8-null mouse jejunum has near-complete absence of several apical markers in the upper 2/3 of the villus (Ameen et al., 2001), while the colon has a generalized alteration in the entire epithelium with reorganization and accompanying patchy distribution of several apical and basolateral markers. Mistargeting of the bile canalicular transmembrane enzyme ecto-ATPase in K8-null hepatocytes from a preferentially apical to a mixed apical-basolateral distribution also occurs (Satoh et al., 1999; Ameen et al., 2001). These distribution differences may share the common feature of mistargeting, with variable degrees of severity. The mechanism of how such mistargeting may occur requires resolution, but interference of keratin interactions with microtubules or other cytoskeletal elements (Chou et al., 2001; Liovic et al., 2003) is possible.

Although mistargeting of membrane proteins in the colon of K8-null mice is relatively generalized, the direct or indirect consequences result in modulation of Na and Cl transport and diarrhea, which precede hyperproliferation and inflammation. These observations indicate a novel function of keratins in the colon. Of potential relevance, epidermal keratins appear to be important for skin barrier function, as suggested by findings in patients with epidermolytic hyperkeratosis (due to K1/K10 mutations), which demonstrate a threefold increase in baseline trans-epidermal water loss rates (Schmuth et al., 2001). The novel involvement of keratins in ion transport may be supported by the I_{sc}, Na, and Cl net fluxes in K8+/− mice, which did not have measurable diarrhea, but that were intermediate between WT and K8-null mice. This suggests a dose effect of keratin depletion such that expression of only one allele may cause subtle changes in Na/Cl transport. The observed mistargeting phenotype may also explain the poorly understood increased susceptibility of K8-null (Caulin et al., 2000; Gilbert et al., 2001) or dominant-negative K18 mutant (Ku et al., 2003b) mouse hepatocytes to apoptosis.

Materials and methods

Antibodies

We used rabbit Abs to ENaCγ (provided by C. Canessa, Yale University), colonic H,K-ATPase β subunit (Sangan et al., 1999), 8592 to K8/18 (Zhou et al., 2003), or AE1/2 Ab 5288 (provided by R. Kopito, Stanford University; Thomas et al., 1989); and rat mAbs to mouse K8 (Troma I; Developmental Studies Hybridoma Bank, University of Iowa), mouse K19 (Troma III; provided by T. Magin, University of Bonn, Bonn, Germany), and mouse anti-PCNA Ab1 (Neomarkers). Texas red or FITC-conjugated phalloidin was used for F-actin staining, and nuclei were stained with Toto-3 or Yo-Pro (Molecular Probes).

Animals and stool analysis

K8+/−, −/−, and +/+ littermates were generated by interbreeding of K8+/− mice (in an FVB/n background) and genotyped (Baribault et al., 1994). Young (1–2 or 14 d old) or adult (2–6 mo old) mice were studied. Stool was collected (5 hourly collections/group) from six mice (5–6 mo old; 3 male, 3 female/genotype) that were housed in metabolic cages, and then weighed (wet weight). The stool was oven dried (95°C, 12 h), re-

weighed (dry weight), and then percent hydration was calculated ([wet − dry weight]/wet weight × 100).

Flux studies

Active Na and Cl transport was measured across isolated distal colonic mucosa in lucite chambers (Binder and Rawlins, 1973; Krishnan et al., 1999). In brief, distal colon was excised and flushed with oxygenated Ringer solution (pH 7.4, 4°C). The colon was cut open and 1–2-cm pieces of unstripped distal colon were mounted in flux chambers (6 mm inner diameter) and bathed in appropriate Ringer solutions (37°C, continuously gassed with a 95% O_2–5% CO_2 mixture). Na-free and Cl-free solutions were prepared by substituting Na and Cl with *N*-methyl-D-glucamine or isethionate, respectively. The potential difference (P.D.) and short circuit current (I_{sc}) were measured, and conductance (G) was calculated using Ohm's law. G and I_{sc} were corrected for the surface area of the lucite chambers. Unidirectional Na and Cl fluxes were measured using ^{22}Na and ^{36}Cl tracers under voltage-clamp conditions. Net fluxes were calculated from the difference between oppositely directed mucosa-to-serosa and serosa-to-mucosa fluxes across tissue pairs that were matched on the basis of differences in initial conductance (<10%). In all experiments, two 15-min flux periods (after a 15-min initial equilibration) were combined to obtain a single flux value for each tissue pair (similarly performed using Na-free or Cl-free bath solutions). In Na substitution experiments, initial I_{sc} and ^{36}Cl fluxes were measured with Na-free mucosal solution, and then the mucosal solution was replaced with Na-containing solution.

Paracellular transport was studied using the nonabsorbable marker [^{14}C]urea. Fluxes were performed under open-circuit conditions. The effect of transport inhibitors on I_{sc} was examined following basal I_{sc} measurements by adding amiloride (100 μM, to mucosal bath) to inhibit the ENaC family of Na channels; dibutyryl cAMP (1 mM) to stimulate Cl secretion through CFTR in the crypt apical membrane; bumetanide (100 μM, to serosal bath) to inhibit basolateral Na-K-2Cl cotransport (and consequently Cl secretion); or 5′-nitro-2-(3-phenylpropylamino)-benzoic acid (NPPB; 50 μM, mucosal bath) to inhibit apical membrane Cl channels.

Surface cell preparation and pH_i measurements

A ~0.5 cm^2 patch of distal colon was placed between two concentric Teflon® O-rings (E.W. Wright, Inc.), immersed in a 250-μl chamber at 37°C, and mounted on an inverted microscope (IX-70; Olympus America, Inc.) equipped for epi-illumination to live-image surface epithelial cells within intact mucosa (Rajendran et al., 1998). Ringer buffer continuously superfused serosal and mucosal aspects and was delivered through a zero-dead-space manifold (Warner Instruments). Surface cells were loaded for 30 min with the pH-sensitive dye BCECF (2′,7′-bis-[2-carboxyethyl]-5-[and-6]-carboxyfluorescein) by switching the solution to a Ringer containing 10 μM BCECF-AM (2′,7′-bis-[2-carboxyethyl]-5-[and-6]-carboxyfluorescein-acetoxymethyl) (Molecular Probes; Rink et al., 1982). Ringer solutions were the same as those used for the flux studies except that the Cl-free solution was prepared using gluconate. High-K^+/nigericin calibration solution contained 10 μM nigericin, 105 mM KCl, 1.0 mM $CaCl_2$, 1.2 mM $MgSO_4$, 2 mM H_3PO_4, 10.5 mM dextrose, 32.2 mM Hepes, 46.4 mM NMDG (pH adjusted with HCl or NMDG). Fluorescence emission was monitored at 530 nm while alternately exciting the dye at 440 and 490 nm using a cooled CCD-based imaging system (Merlin®; PerkinElmer). Image pairs were obtained every 5 s, and, using image analysis software, pixels within the boundaries of individual surface cells were grouped. For each cell in each sample, I_{490}/I_{440} was determined, and each experiment was concluded with a single-point calibration using the nigericin/high-K^+ technique, clamping pH_i at 7.00 (Chaillet et al., 1986; Singh et al., 1995).

Tissue processing, immunoblotting, and microscopy

Distal colon was excised, rinsed, and then (a) snap-frozen in liquid N_2 for subsequent biochemical analyses, (b) immediately fixed in 10% formalin for hematoxylin and eosin staining (Histo-tec Laboratory; Hayward, CA), or fixed in 2% glutaraldehyde for electron microscopy analysis (Toivola et al., 2000), or (c) embedded in O.C.T. compound (Miles Inc.) and then rapidly frozen for subsequent cryosectioning and Ab staining (Toivola et al., 2000). For 1–14-d-old mice, the entire colon was used for biochemical analysis and immunofluorescence.

Total cell lysates were prepared for SDS-PAGE and immunoblotting (Toivola et al., 2000). Goblet cell size was estimated from electron micrographs of identical magnification. Micrographs were copied onto paper, and individual goblet cells or mucus vacuoles were cut out and then weighed, followed by conversion of the weight (grams) to surface area (μm^2). Continuity of F-actin along the luminal epithelium was assessed using 25 images of F-actin–stained tissues (where the entire luminal epithelium could be distinguished) from three mice/genotype (40x objective, MRC1024ES confocal microscope, and Lasersharp software; BioRad). The percent of F-actin gaps (areas lacking F-actin staining) was calculated for each image as ([length of actin gaps/total length of analyzed surface epithelium] × 100).

Colonocyte isolation and cell viability

Colonocyte/crypt units were isolated based on a method for rat colon (Roediger and Truelove, 1979). In brief, Krebs Hensleit buffers (25 mM $NaHCO_3$, 11.8 mM NaCl, 4.7 mM KCl, 1.2 mM $MgSO_4$, 1.2 mM NaH_2PO_4, pH 7.4, 37°C) without (KH-Ca) or with (KH+Ca) 1.2 mM $CaCl_2$ calcium were prepared and oxygenated. The entire colon was excised and gently flushed with KH-Ca. A thread (3–0 Plain gut; United States Surgical) was pushed through the intestine, a knot tied around one end, and the intestine inverted. The intestine, now with the epithelium facing out, was inflated with KH-Ca/0.25% BSA, and the other end ligated. The colon was place in KH-Ca/5 mM EDTA/0.25% BSA, stirred (37°C, Dubnoff shaker, 70 oscillations/min, 25 min), gently rinsed with KH+Ca, and then vigorously shaken (1 min) in KH-Ca/0.25% BSA. Collected cells were pelleted (1,500 rpm, 5 min) and washed twice (1,000 rpm, 3 min, 22°C) with oxygenated KH+Ca/2.5% BSA. Cell viability was determined by trypan blue exclusion and by LDH releases (BioVision) as percent of total LDH.

Statistical analysis

Numerical data for stool hydration, goblet cell size, and mucus content were compared using two-tailed *t* test. One-tailed *t* test was used for surface cell pH measurements. Flux data were analyzed using unpaired *t* test, and paired *t* test was used to compare the change in I_{sc} after cAMP addition between WT and K8-null groups, and Wilcoxon Signed Ranks nonparametric analysis to calculate significance between control and +cAMP time periods. Mouse weights were analyzed using a one-sided randomized block permutation test.

We are very grateful to Helene Baribault (Tularik, South San Francisco, CA) for providing the K8-null mice, Cecilia Canessa for anti-ENaC antibodies, Thomas Magin for the Troma III antibody, Ron Kopito for the anti-AE1/2 antibodies, Aida Habtezion for helpful discussions, Kris Morrow and Kurt Campbell for assistance with figure preparation, George Chang and Richard Olshen (Stanford University, Department of Statistics) for statistical analysis, Evelyn Resurreccion for sectioning and fluorescence staining, and Steve Avolicino for histology staining.

This work was supported by VA Merit Award and National Institutes of Health (NIH) grant DK52951 (M.B. Omary); NIH Digestive Disease Center grant DK56339 (Stanford University); NIH grants DK18777 and DK60069 (H.J. Binder); and NIH grant DK02410 and an ADHF/AGA Miles and Shirley Fiterman Basic Research Award (S.K. Singh).

Submitted: 19 August 2003
Accepted: 5 February 2004

References

Ahn, Y.J., D.R. Brooker, F. Kosari, B.J. Harte, J. Li, S.A. Mackler, and T.R. Kleyman. 1999. Cloning and functional expression of the mouse epithelial sodium channel. *Am. J. Physiol.* 277:F121–F129.

Alper, S.L., R.B. Darman, M.N. Chernova, and N.K. Dahl. 2002. The AE gene family of Cl/HCO3- exchangers. *J. Nephrol.* 15(Suppl 5):S41–S53.

Alvarez de la Rosa, D., C.M. Canessa, G.K. Fyfe, and P. Zhang. 2000. Structure and regulation of amiloride-sensitive sodium channels. *Annu. Rev. Physiol.* 62:573-594.

Ameen, N.A., Y. Figueroa, and P.J. Salas. 2001. Anomalous apical plasma membrane phenotype in CK8-deficient mice indicates a novel role for intermediate filaments in the polarization of simple epithelia. *J. Cell Sci.* 114:563–575.

Baribault, H., J. Penner, R.V. Iozzo, and M. Wilson-Heiner. 1994. Colorectal hyperplasia and inflammation in keratin 8-deficient FVB/N mice. *Genes Dev.* 8:2964–2973.

Baribault, H., J. Price, K. Miyai, and R.G. Oshima. 1993. Mid-gestational lethality in mice lacking keratin 8. *Genes Dev.* 7:1191–1202.

Barrett, K.E., and S.J. Keely. 2000. Chloride secretion by the intestinal epithelium: molecular basis and regulatory aspects. *Annu. Rev. Physiol.* 62:535–572.

Binder, H., and G. Sandle. 1994. Electrolyte transport in the mammalian colon. *In* Physiology of the Gastrointestinal Tract. L.R. Johnson, editor. Raven Press, New York. 2133–2171.

Binder, H.J., and C.L. Rawlins. 1973. Effect of conjugated dihydroxy bile salts on

electrolyte transport in rat colon. *J. Clin. Invest.* 52:1460–1466.

Bischof, G., E. Cosentini, G. Hamilton, M. Riegler, J. Zacherl, B. Teleky, W. Feil, R. Schiessel, T.E. Machen, and E. Wenzl. 1996. Effects of extracellular pH on intracellular pH-regulation and growth in a human colon carcinoma cell-line. *Biochim. Biophys. Acta.* 1282:131–139.

Boron, W.F. 1992. Control of intracellular pH. *In* The Kidney: Physiology and Pathophysiology. D.W. Seldin, Giebisch, G., editor. Raven Press, New York. 219–263.

Caulin, C., C.F. Ware, T.M. Magin, and R.G. Oshima. 2000. Keratin-dependent, epithelial resistance to tumor necrosis factor- induced apoptosis. *J. Cell Biol.* 149:17–22.

Chaillet, J.R., K. Amsler, and W.F. Boron. 1986. Optical measurements of intracellular pH in single LLC-PK1 cells: demonstration of Cl-HCO_3 exchange. *Proc. Natl. Acad. Sci. USA.* 83:522–526.

Chou, Y.H., B.T. Helfand, and R.D. Goldman. 2001. New horizons in cytoskeletal dynamics: transport of intermediate filaments along microtubule tracks. *Curr. Opin. Cell Biol.* 13:106–109.

Coulombe, P.A., and M.B. Omary. 2002. 'Hard' and 'soft' principles defining the structure, function and regulation of keratin intermediate filaments. *Curr. Opin. Cell Biol.* 14:110–122.

Cuffe, J.E., M. Bertog, S. Velazquez-Rocha, O. Dery, N. Bunnett, and C. Korbmacher. 2002. Basolateral PAR-2 receptors mediate KCl secretion and inhibition of Na^+ absorption in the mouse distal colon. *J. Physiol.* 539:209–222.

Cuthbert, A.W., M.E. Hickman, and L.J. MacVinish. 1999. Formal analysis of electrogenic sodium, potassium, chloride and bicarbonate transport in mouse colon epithelium. *Br. J. Pharmacol.* 126:358–364.

Davies, R.J., H. Asbun, S.M. Thompson, D.A. Goller, and G.I. Sandle. 1990. Uncoupling of sodium chloride transport in premalignant mouse colon. *Gastroenterology.* 98:1502–1508.

Fuchs, E., and K. Weber. 1994. Intermediate filaments: structure, dynamics, function, and disease. *Annu. Rev. Biochem.* 63:345–382.

Gilbert, S., A. Loranger, N. Daigle, and N. Marceau. 2001. Simple epithelium keratins 8 and 18 provide resistance to Fas-mediated apoptosis. The protection occurs through a receptor-targeting modulation. *J. Cell Biol.* 154:763–774.

Greig, E.R., E.H. Baker, T. Mathialahan, R.P. Boot-Handford, and G.I. Sandle. 2002. Segmental variability of ENaC subunit expression in rat colon during dietary sodium depletion. *Pflugers Arch.* 444:476–483.

Hofer, D., T. Jons, J. Kraemer, and D. Drenckhahn. 1998. From cytoskeleton to polarity and chemoreception in the gut epithelium. *Ann. NY Acad. Sci.* 859: 75–84.

Hosokawa, M., H. Tsukada, T. Saitou, M. Kodama, M. Onomura, H. Nakamura, K. Fukuda, and Y. Seino. 1998. Effects of okadaic acid on rat colon. *Dig. Dis. Sci.* 43:2526–2535.

Irvine, A.D., and W.H. McLean. 1999. Human keratin diseases: the increasing spectrum of disease and subtlety of the phenotype-genotype correlation. *Br. J. Dermatol.* 140:815–828.

Jacob, R., K.P. Zimmer, J. Schmitz, and H.Y. Naim. 2000. Congenital sucrase-isomaltase deficiency arising from cleavage and secretion of a mutant form of the enzyme. *J. Clin. Invest.* 106:281–287.

Jaquemar, D., S. Kupriyanov, M. Wankell, J. Avis, K. Benirschke, H. Baribault, and R.G. Oshima. 2003. Keratin 8 protection of placental barrier function. *J. Cell Biol.* 161:749–756.

Kere, J., and P. Hoglund. 2000. Inherited disorders of ion transport in the intestine. *Curr. Opin. Genet. Dev.* 10:306–309.

Krishnan, S., B.S. Ramakrishna, and H.J. Binder. 1999. Stimulation of sodium chloride absorption from secreting rat colon by short-chain fatty acids. *Dig. Dis. Sci.* 44:1924–1930.

Ku, N.O., J.M. Darling, S.M. Krams, C.O. Esquivel, E.B. Keeffe, R.K. Sibley, Y.M. Lee, T.L. Wright, and M.B. Omary. 2003a. Keratin 8 and 18 mutations are risk factors for developing liver disease of multiple etiologies. *Proc. Natl. Acad. Sci. USA.* 100:6063–6066.

Ku, N.O., R.M. Soetikno, and M.B. Omary. 2003b. Keratin mutation in transgenic mice predisposes to Fas but not TNF-induced apoptosis and massive liver injury. *Hepatology.* 37:1006–1014.

Kunzelmann, K., and M. Mall. 2002. Electrolyte transport in the mammalian colon: mechanisms and implications for disease. *Physiol. Rev.* 82:245–289.

Liovic, M., M.M. Mogensen, A.R. Prescott, and E.B. Lane. 2003. Observation of keratin particles showing fast bidirectional movement colocalized with microtubules. *J. Cell Sci.* 116:1417–1427.

Loranger, A., S. Duclos, A. Grenier, J. Price, M. Wilson-Heiner, H. Baribault, and N. Marceau. 1997. Simple epithelium keratins are required for maintenance of hepatocyte integrity. *Am. J. Pathol.* 151:1673–1683.

Moll, R., W.W. Franke, D.L. Schiller, B. Geiger, and R. Krepler. 1982. The catalog of human cytokeratins: patterns of expression in normal epithelia, tumors and cultured cells. *Cell.* 31:11–24.

Omary, M.B., N.O. Ku, and D.M. Toivola. 2002. Keratins: guardians of the liver. *Hepatology.* 35:251–257.

Rajendran, V.M., and H.J. Binder. 2000. Characterization and molecular localization of anion transporters in colonic epithelial cells. *Ann. NY Acad. Sci.* 915: 15–29.

Rajendran, V.M., S.K. Singh, J. Geibel, and H.J. Binder. 1998. Differential localization of colonic H(+)-K(+)-ATPase isoforms in surface and crypt cells. *Am. J. Physiol.* 274:G424–G429.

Rink, T.J., R.Y. Tsien, and T. Pozzan. 1982. Cytoplasmic pH and free Mg^{2+} in lymphocytes. *J. Cell Biol.* 95:189–196.

Roediger, W.E., and S.C. Truelove. 1979. Method of preparing isolated colonic epithelial cells (colonocytes) for metabolic studies. *Gut.* 20:484–488.

Sangan, P., S.S. Kolla, V.M. Rajendran, M. Kashgarian, and H.J. Binder. 1999. Colonic H-K-ATPase beta-subunit: identification in apical membranes and regulation by dietary K depletion. *Am. J. Physiol.* 276:C350–C360.

Satoh, M.I., H. Hovington, and M. Cadrin. 1999. Reduction of cytochemical ecto-ATPase activities in keratin 8-deficient FVB/N mouse livers. *Med. Electron Microsc.* 32:209–212.

Schmuth, M., G. Yosipovitch, M.L. Williams, F. Weber, H. Hintner, S. Ortiz-Urda, K. Rappersberger, D. Crumrine, K.R. Feingold, and P.M. Elias. 2001. Pathogenesis of the permeability barrier abnormality in epidermolytic hyperkeratosis. *J. Invest. Dermatol.* 117:837–847.

Schultheis, P.J., L.L. Clarke, P. Meneton, M.L. Miller, M. Soleimani, L.R. Gawenis, T.M. Riddle, J.J. Duffy, T. Doetschman, T. Wang, et al. 1998. Renal and intestinal absorptive defects in mice lacking the NHE3 Na^+/H^+ exchanger. *Nat. Genet.* 19:282–285.

Schulz-Baldes, A., S. Berger, F. Grahammer, R. Warth, I. Goldschmidt, J. Peters, G. Schutz, R. Greger, and M. Bleich. 2001. Induction of the epithelial Na^+ channel via glucocorticoids in mineralocorticoid receptor knockout mice. *Pflugers Arch.* 443:297–305.

Sellin, J.H., A. Hall, E.J. Cragoe, Jr., and W.P. Dubinsky. 1993. Characterization of an apical sodium conductance in rabbit cecum. *Am. J. Physiol.* 264:G13–G21.

Shrode, L.D., H. Tapper, and S. Grinstein. 1997. Role of intracellular pH in proliferation, transformation, and apoptosis. *J. Bioenerg. Biomembr.* 29:393–399.

Singh, S.K., H.J. Binder, J.P. Geibel, and W.F. Boron. 1995. An apical permeability barrier to NH^3/NH^{4+} in isolated, perfused colonic crypts. *Proc. Natl. Acad. Sci. USA.* 92:11573–11577.

Spicer, Z., L.L. Clarke, L.R. Gawenis, and G.E. Shull. 2001. Colonic H(+)-K(+)-ATPase in K(+) conservation and electrogenic Na(+) absorption during Na(+) restriction. *Am. J. Physiol. Gastrointest. Liver Physiol.* 281:G1369–G1377.

Strober, W., I.J. Fuss, and R.S. Blumberg. 2002. The immunology of mucosal models of inflammation. *Annu. Rev. Immunol.* 20:495–549.

Thomas, H.A., T.E. Machen, A. Smolka, R. Baron, and R.R. Kopito. 1989. Identification of a 185-kDa band 3-related polypeptide in oxyntic cells. *Am. J. Physiol.* 257:C537–C544.

Toivola, D.M., M.B. Omary, N.O. Ku, O. Peltola, H. Baribault, and J.E. Eriksson. 1998. Protein phosphatase inhibition in normal and keratin 8/18 assembly-incompetent mouse strains supports a functional role of keratin intermediate filaments in preserving hepatocyte integrity. *Hepatology.* 28:116–128.

Toivola, D.M., H. Baribault, T. Magin, S.A. Michie, and M.B. Omary. 2000. Simple epithelial keratins are dispensable for cytoprotection in two pancreatitis models. *Am. J. Physiol. Gastrointest. Liver Physiol.* 279:G1343–G1354.

Toivola, D.M., M.I. Nieminen, M. Hesse, T. He, H. Baribault, T.M. Magin, M.B. Omary, and J.E. Eriksson. 2001. Disturbances in hepatic cell-cycle regulation in mice with assembly-deficient keratins 8/18. *Hepatology.* 34: 1174–1183.

Wenzl, E., M.D. Sjaastad, W.H. Weintraub, and T.E. Machen. 1989. Intracellular pH regulation in IEC-6 cells, a cryptlike intestinal cell line. *Am. J. Physiol.* 257:G732–G740.

Zatloukal, K., C. Stumptner, M. Lehner, H. Denk, H. Baribault, L.G. Eshkind, and W.W. Franke. 2000. Cytokeratin 8 protects from hepatotoxicity, and its ratio to cytokeratin 18 determines the ability of hepatocytes to form Mallory bodies. *Am. J. Pathol.* 156:1263–1274.

Zhou, Q., D.M. Toivola, N. Feng, H.B. Greenberg, W.W. Franke, and M.B. Omary. 2003. Keratin 20 helps maintain intermediate filament organization in intestinal epithelia. *Mol. Biol. Cell.* 14:2959–2971.